THE JOURNAL OF PHYSICAL CHEMISTRY Letters

Letter

pubs.acs.org/JPCL

# Probing Coster–Kronig Transitions in Aqueous $Fe^{2+}$ Solution Using Inverse Partial and Partial Fluorescence Yield at the L-Edge

Malte D. Gotz,[†,‡] Mikhail A. Soldatov,[†,§] Kathrin M. Lange,[†,‡] Nicholas Engel,[†,‡] Ronny Golnak,[†] René Könnecke,[†] Kaan Atak,[†] Wolfgang Eberhardt,[∥] and Emad F. Aziz*[,†,‡]

[†]Helmholtz-Zentrum Berlin für Materialien und Energie, Albert-Einstein-Strasse 15, 12489 Berlin, Germany

[‡]Department of Physics, Freie Universität Berlin, Arnimallee 14, 14195 Berlin, Germany

[§]Research Center for Nanoscale Structure of Matter, Southern Federal University, Sorge 5, Rostov-na-Donu 344090, Russia

[∥]Institute of Optic and Atomic Physics, Technische Universität Berlin, Strasse des 17. Juni 135, 10623 Berlin, Germany

Supporting Information

**ABSTRACT:** Specific Coster–Kronig (CK) transitions in 3d transition metals are close to the threshold of energetic possibility, being disallowed in free atoms, while possible in solids. Moreover, they have been shown to be quite sensitive to chemical bonding. Nevertheless, there has been no direct study of such behavior in solution. Here we present an approach to quantify such transitions in solution, by comparing relative fluorescence of different edges to their relative absorption strengths. The difficulties of acquiring a measurement of the absorption in solution are overcome by applying the recently developed method of inverse partial fluorescence yield to a liquid sample using the microjet. This method has been demonstrated on solids to be bulk sensitive and able to obtain absorption spectra free of self-absorption or saturation effects. We extend this approach to investigate the L-edge of aqueous $Fe^{2+}$ using a combination of a soft X-ray light source and a high-resolution X-ray emission spectrometer.

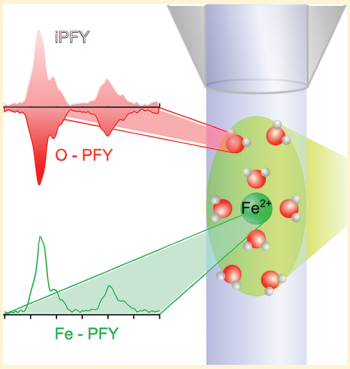


**SECTION:** Spectroscopy, Photochemistry, and Excited States

The absorption of an X-ray photon of appropriate energy creates a core-hole in the respective molecular orbital, which subsequently decays through multiple possible channels such as Auger-decay and fluorescence. Coster–Kronig (CK) transitions[1] are a particular kind of Auger decay where a core-hole is filled by an electron from the same shell while excess energy is dissipated through ejection of a higher lying electron. For the L-edge X-ray absorption of a transition metal (TM), the resulting $L_2$ core-hole can be filled by an $L_3$ electron under ejection of an $M_{4,5}$ electron ($L_2$–$L_3M_{4,5}$). A schematic for the L-edge X-ray absorption, emission, and CK processes is presented in Figure 1. Any such transition must fulfill energy conservation. In the case of the $L_2$–$L_3M_{4,5}$ CK transition, the energy of the primary $L_2$ core-hole has to be larger than the sum of the secondary $L_3$ and $M_{4,5}$ core-holes. Since core-holes of the same shell have a small energy difference, CK transitions are only possible if a correspondingly shallow core-hole can be created (see Figure 1e,f). At the same time, due to the strong overlap of the core wave functions, the CK process often becomes the dominating decay channel if permissible.[2] Particularly for 3d TM, the $L_2$–$L_3M_{4,5}$ CK transition does not take place in free atoms, while it can be observed in solid metal.[3,4] This pronounced difference arises from screening effects in the solid, which lower the energy of valence-holes and, correspondingly, the binding energy of those electrons.[5] Similarly, CK transitions were shown to be quite sensitive to chemical bonding in 3d TMs.[6,7] The near threshold sensitivity of the CK transition makes it a potential tool for investigating the effect of the surrounding atoms on the probed element. Qualitative and quantitative studies have been performed to analyze the CK process from the $L_2/L_3$ emission intensity ratio in 3d TMs.[8−12] Yet, observations of CK transitions have hitherto been limited to solids and gases, while, here, we present the first study in solution, observing CK transitions of dissolved $Fe^{2+}$ ions from a $FeCl_2$ solution in water. Beyond the sensitive behavior with respect to CK transitions, 3d TMs are of more general interest due to their variety of functions as catalysts and their key role in biology as active centers of proteins.[13]

Figure 1c–f illustrates the electronic transitions involved in L-edge absorption and fluorescence of a TM in water. Incident photons cause 2p–3d electron transitions at the resonance energy of a TM (Figure 1c, left), and oxygen 1s ionization of $H_2O$ (Figure 1c, right). The number of created core-holes is assumed to be linearly dependent on the absorption cross-section of the TM L-edge because the cross-section of water ionization is nearly constant once the excitation energy is well above its threshold of 538.1 eV.[14] The relaxation of electrons into these holes (Figure 1d) causes emission of fluorescence

**Received:** April 3, 2012
**Accepted:** May 29, 2012
**Published:** May 29, 2012





dx.doi.org/10.1021/jz300403n | J. Phys. Chem. Lett. 2012, 3, 1619–1623

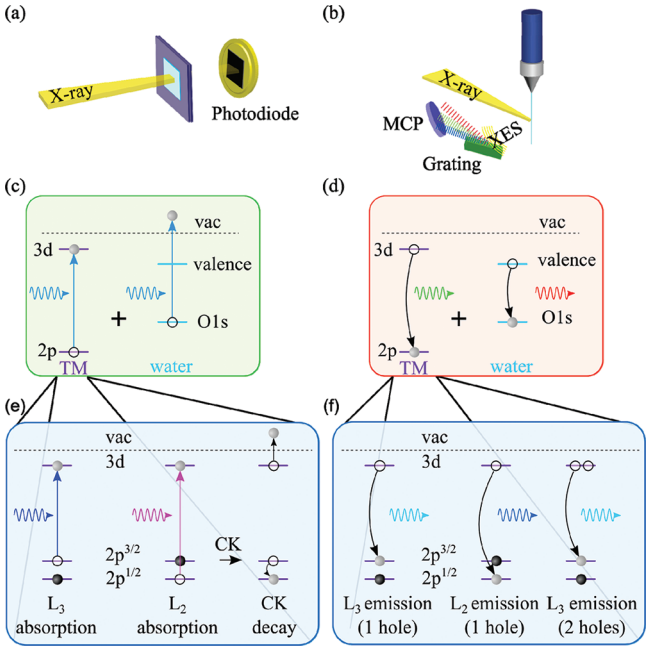


**Figure 1.** (a,b) Experimental setup of a transmission and a fluorescence measurement. (c) Highly reduced energy level scheme for the L-edge absorption of a TM in water and (d) subsequent radiative decay. (e,f) Core-hole decay, in more detail, for the TM with the possibility of a CK transition and the resulting fluorescence.

photons. Moreover a $L_2$-core-hole can first decay in a nonradiative CK process to a double hole state $L_3M_{4,5}$ (Figure 1e), which in turn will also emit fluorescence (Figure 1f).

The probability of the $L_2$–$L_3M_{4,5}$ CK transition ($f_{2,3}$) can be estimated in a simplified picture, if one measures the fluorescence from the two iron fine-structure lines separately ($L_3$–$M_{4,5}$ and $L_2$–$M_{4,5}$), while exciting at the $L_2$- or the $L_3$-absorption-edge. The fluorescence from the $L_3$–$M_{4,5}$ line while exciting the $L_3$ edge is given by

$$FY_{L_3} = \mu_{L_3}\omega_{L_3} \tag{1}$$

Where $\mu_{L_3}$ denotes the linear attenuation coefficient at the $L_3$-edge, creating $L_3$-core-holes, and $\omega_{L_3}$ is the probability of fluorescence decay of those core-holes. The fluorescence from the same line while exciting the $L_2$-edge is

$$FY_{ck} = \mu_{L_2} f_{2,3} \omega_{L_3M_{4,5}} \tag{2}$$

Where $\mu_{L_2}$ denotes the linear attenuation coefficient at the $L_2$-edge creating $L_2$-core-holes, $f_{2,3}$ is the CK probability, and $\omega_{L_3M_{4,5}}$ is the fluorescence probability of the two-hole $L_3M_{4,5}$ state. Dividing each equation by the linear attenuation coefficient determined via iPFY and forming the quotient of the two equations leads to

$$\frac{FY_{L_3}\mu_{L_2}}{FY_{ck}\mu_{L_3}} = \frac{\omega_{L_3M_{4,5}}}{\omega_{L_3}} f_{2,3} \tag{3}$$

If the two fluorescence probabilities ($\omega_{L_3}$ and $\omega_{L_3M_{4,5}}$) are assumed equal, the CK transition rate is given by the ratio of the fluorescence intensity at the two edges, as well as the ratio of the linear attenuation coefficients, i.e., the X-ray absorption.

L-edge X-ray absorption spectroscopy (XAS) of TM is also in general a powerful tool, because it provides information about the electronic configuration of the unoccupied states involved in chemical bonding and charge transfer dynamics.[15−21] The transmission approach to XAS as illustrated in Figure 1a is difficult in the soft X-ray range of the L-edges of TM (500−1000 eV), due to the rapid attenuation of soft X-ray photons in matter. A penetration depth of 1−2 $\mu$m[22] in liquid requires an appropriately thin sample to be prepared between two thin transparent membranes.[20] Such a technique is prone to sample damage, especially in the case of sensitive biochemical materials. Alternatively, for obtaining an absorption spectrum without the difficulties of mircometer-thin sample preparation, total fluorescence yield (TFY) or partial fluorescence yield (PFY) measurements are often used.[22] The experimental geometry is shown in Figure 1b. TFY and PFY rely on the proportionality of the emitted fluorescence to the number of created core-holes and, if such proportionality is ensured, can provide spectra proportional to the transmission XAS for very dilute samples.[18,23] Both will be affected by saturation/self-absorption effects, which depend on the sample concentration.[24,25]

A method free of the artifacts in TFY and PFY was recently developed by Achkar et al.[26] In what they termed "inverse partial fluorescence yield" (iPFY), one uses the fact that the fluorescence of a lower-energy transition, which is not resonantly excited, is reduced, and the reduction is inversely proportional to the absorption of the resonant excitation. Spectra obtained using this method were shown to agree very well with those obtained from total electron yield (TEY) measurements for a solid sample. Therefore, the requirement of a dilute limit as imposed on TFY or PFY measurements is not necessary here. The iPFY approach requires the presence of an observer element in the sample, which has an energetically lower lying absorption edge than the element of interest so that it is nonresonantly excited throughout the investigated energy range. For aqueous $Fe^{2+}$, the oxygen K-edge of water is a suitable observer, as its strong fluorescence is readily measured. Variations in the absorption strength of the sample while scanning the iron L-edge alter the number of photons available for the absorption by oxygen, in turn altering the oxygen fluorescence. Accordingly, the oxygen fluorescence is reduced when the iron L-edge absorbs stronger and vice versa. Inverting the oxygen fluorescence then allows a measurement of the L-edge's absorption strength (see the work of Achkar et al.[26] or the Supporting Information).

Figure 2a shows a comparison between the PFY from the $Fe^{2+}$ ions and their absorption determined from the iPFY of oxygen. The spectra are normalized in order to allow a comparison across the orders of magnitude separating the iPFY signal and the direct fluorescence signal. The raw data is measured as counts on a CCD camera; each energy point of a PFY spectrum is obtained through summation of all counts occurring on a specified area on the CCD camera. The thereby acquired PFY spectra exhibit background trends due to changing experimental conditions such as rising vacuum pressure. The data is corrected for those trends by fitting a third-order polynomial as a background.

The Fe-PFY differs from the O-iPFY in two main points: The Fe-PFY is broadened at the $L_3$ peak, and the overall fluorescence probability at $L_2$ appears higher. Both are explained by saturation,[24] which roughly reduces the major peaks intensity, thus relatively broadening the features. Saturation should not be present in a dilute sample if the background absorption is much stronger than the edge under


dx.doi.org/10.1021/jz300403n | J. Phys. Chem. Lett. 2012, 3, 1619−1623

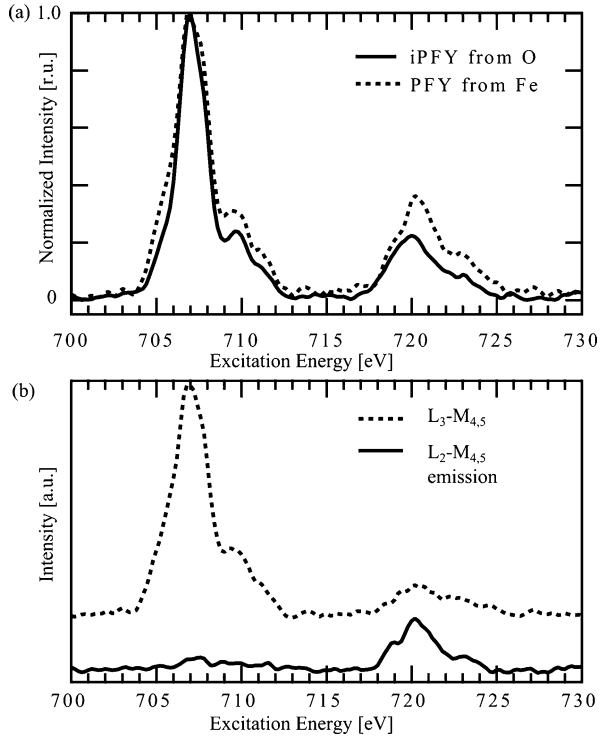


**Figure 2.** Measurements form 1 M $FeCl_2$ solution in water. (a) Comparison between oxygen iPFY (directly proportional to absorption) and the distorted iron PFY spectrum at the L-edge. (b) Iron PFY dissected into contribution from the different core-holes.

investigation ($\mu_{\text{background}} \gg \mu_{\text{edge}}$). For $Fe^{2+}$, a 1 M concentration is still too high, though, to be considered dilute, as evidenced by the saturation and further shown in our Supporting Information.

Figure 2b presents the PFY spectra from $Fe^{2+}$ ions separated into contributions from $L_2$- and $L_3$-holes. The spectra are the result of limiting the energy integration of the emission to either the $L_2-M_{4,5}$ or the $L_3-M_{4,5}$ emission line. The significant $L_3-M_{4,5}$ emission at the $L_2$ resonance shows presence of $L_3$ holes, which cannot stem from nonresonant excitation, because such slowly varying contributions were eliminated in the background correction. This emission is a result of $L_2-L_3M_{4,5}$ CK decay following the creation of an $L_2$-core-hole. Accordingly, here we present an indirect observation of CK-decay in liquid phase of aqueous $Fe^{2+}$, which adds to explaining the variation in fluorescence yield at the $L_2$-edge by another contribution beyond saturation. While the CK process leaves behind one $L_3$ hole for every $L_2$ hole, it also creates an extra vacancy in the M-shell illustrated in Figure 1e,f. This additional vacancy decreases the screening of the core-hole, affecting the ratio of Auger to fluorescence decay[10,27] and resulting in a higher fluorescence yield from the $L_2$-edge than the $L_3$-edge.

Returning to eq 3, we can utilize the PFY data from Figure 2b to obtain the ratio $FY_{L_3}/FY_{ck}$ and the iPFY data from Figure 2a to calculate $\mu_{L_2}/\mu_{L_3}$ and thus estimate the CK probability. As a caveat, we should point out that eqs 1 and 2 do not take the effects of saturation and reabsorption on the measured signal into account. By forming the quotient for all available energy points in eq 3, we aim to minimize this inaccuracy. Averaging over the points yields the CK-transition rate, and the standard deviation is taken as an estimate of this approximation's error . Because of the aforementioned inequality of the fluorescence probability of the double- and single-hole states ($\omega_{L_3M_{4,5}} > \omega_{L_3}$), we take this as an upper limit of the CK-transition rate:

$$f_{2,3} < 0.48 \pm 0.18$$

For pure, metallic iron, Kurmaev et al.[11] estimate $f_{2,3} = 0.42$ theoretically, in good agreement with their experiment, and Hague et al.[10] inferred a value of $f_{2,3} = 0.5$ for iron from experiments on other elements. It is astonishing that the transition in doubly charged $Fe^{2+}$ ions in solution is about as strong as in Fe metal. This is indicative of a strong interaction of the valence orbitals with the water, giving rise to significant screening effects. The effect appears to be strong enough to reduce the binding energies to levels comparable to uncharged solid states because the CK transition rates are so remarkably close.

In conclusion, we introduced here the use of CK transitions as a probe for the interaction of dissolved ions, and possibly more complex systems with their environment, in solution. Probing the influence of varying ligands or solvents on the CK rate should allow insights into the strength of the chemical bond and ion−solvent interaction. In addition to opening possible new experimental avenues, the existence of CK transitions is important in the interpretation of most X-ray-based spectroscopies. In X-ray emission, CK transitions manifest as satellite lines due to the slightly shifted emission energy of the double-hole state, and variations must be taken into account when interpreting intensity ratios.[11] In Auger and photoelectron spectroscopy, interference effects, in addition to the satellite lines, may play a role due to CK effects.[28,29] Furthermore, we extend the application of iPFY and PFY in solution using the liquid microjet for the first time. This approach allows collection of soft X-ray spectra using a FY technique free from artifacts due to self-absorption and saturation.

## ■ EXPERIMENTAL SECTION

For the presented experiment our recently developed high-resolution X-ray emission spectrometer based on a Rowland-circle design[30,31] was used, which is schematically presented in Figure 3. The experiments were performed at the U-41 PGM

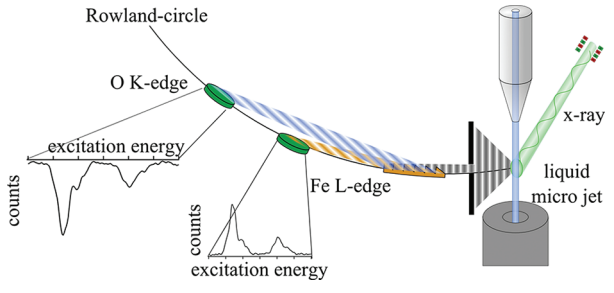


**Figure 3.** Illustration of an XES spectrometer in Rowland-circle design with a microjet for liquid spectroscopy. The different detector positions for first-order oxygen and iron emission are sketched with the resulting spectra, when scanning excitation energy.

beamline at the Helmholtz-Zentrum Berlin (BESSY II synchrotron facility). PFY spectra were obtained by integrating over the appropriate energy interval of the emission spectrum while varying the excitation energy (see Supporting Information Figure S.1). In order to ascertain correct operation the oxygen emission of solid, $Fe_2O_3$-powder was measured and


dx.doi.org/10.1021/jz300403n | J. Phys. Chem. Lett. 2012, 3, 1619−1623

used for calibration. The results after inversion and background correction of the signal are compared to TEY data from the literature[32] in the Supporting Information (Figure S.2) and show the expected agreement. $Fe_2O_3$ was selected due to its low reactivity, reducing the risk of sample deterioration by radiation, due to the availability of data in literature, and due to the similarity to the liquid investigation where oxygen and iron are also mainly involved. The liquid experiment was performed on a microjet of aqueous $Fe^{2+}$ ions from a 1 M $FeCl_2$ solution. To form the microjet, a glass nozzle with an opening of 20 $\mu$m was used. The $FeCl_2$ solution was prepared by dissolving $FeCl_2$ tetrahydrate commercially available from Fluka in purified water and subsequently filtered through a Machery-Nagel 619eh filter to remove any undissolved remains.

## ■ ASSOCIATED CONTENT

### Supporting Information

Detailed reasoning for validity of iPFY as XAS and comparison of iPFY data from $Fe_2O_3$ to literature, and estimation of absorption strengths and XES spectra to illustrate how integration for PFY was chosen. This material is available free of charge via the Internet at http://pubs.acs.org.

## ■ AUTHOR INFORMATION

### Corresponding Author

*E-mail: emad.aziz@helmholtz-berlin.de.

### Notes

The authors declare no competing financial interest.

## ■ ACKNOWLEDGMENTS

We thank Dr. Bernd Winter for fruitful discussions. This work was supported by the Helmholtz-Gemeinschaft via the young investigator fund VH-NG-635 and the European Research Council Grant No. 279344.

## ■ REFERENCES

(1) Coster, D.; Kronig, R. New Type of Auger Effect and Its Influence on the X-ray Spectrum. *Physica* **1935**, *2*, 13−24.
(2) Chen, M. H.; Crasemann, B.; Mark, H. Widths and Fluorescence Yields of Atomic L-Shell Vacancy States. *Phys. Rev. A* **1981**, *24*, 177−182.
(3) Matthew, J. A. D.; Nuttall, J. D.; Gallon, T. E. Enhancement of Coster−Kronig Rates in Solid-State Environments. *J. Phys. C: Solid State* **1976**, *9*, 883−888.
(4) Antonides, E.; Janse, E. C.; Sawatzky, G. A. LMM Auger-Spectra of Cu, Zn, Ga, and Ge 0.2. Relationship with L23 Photoelectron-Spectra Via $L_2L_3M_{45}$ Coster−Kronig Process. *Phys Rev B* **1977**, *15*, 4596−4601.
(5) Antonides, E.; Sawatzky, G. A. $L_2L_3M_{4,5}$ Coster−Kronig Process in Zn and ZnO in Solid-State. *J. Phys. C: Solid State* **1976**, *9*, L547−L552.
(6) Duda, L. C. Magnetic Circular Dichroism in Soft X-ray Emission of Itinerant and Localized Magnets. *J. Electron. Spectrosc.* **2000**, *110*, 287−304.
(7) Butorin, S. M.; Galakhov, V. R.; Kurmaev, E. Z.; Glazyrina, V. I. Soft-X-ray Emission CuL Spectra and Copper-Oxygen Bond Covalency in High-Tc Superconductors. *Solid State Commun.* **1992**, *81*, 1003−1007.
(8) Aksela, S.; Sivonen, J. $L_{2,3}M_{4,5}M_{4,5}$ Principal and Satellite Auger-Spectra of Free Copper Atoms. *Phys. Rev. A* **1982**, *25*, 1243−1246.
(9) Haak, H. W.; Sawatzky, G. A.; Thomas, T. D. Auger-Photoelectron Coincidence Measurements in Copper. *Phys. Rev. Lett.* **1978**, *41*, 1825−1827.
(10) Hague, C. F.; Mariot, J. M.; Guo, G. Y.; Hricovini, K.; Krill, G. Coster−Kronig Contributions to Magnetic Circular-Dichroism in the $L_{2,3}$ X-ray-Fluorescence of Iron. *Phys. Rev. B* **1995**, *51*, 1370−1373.
(11) Kurmaev, E. Z.; Ankudinov, A. L.; Rehr, J. J.; Finkelstein, L. D.; Karimov, P. F.; Moewes, A. The $L_2$:$L_3$ Intensity Ratio in Soft X-ray Emission Spectra of 3d-Metals. *J. Electron. Spectrosc. Relat. Phenom.* **2005**, *148*, 1−4.
(12) Cao, W.; Dousse, J. C.; Hoszowska, J.; Zitnik, M.; Kavcic, M.; Bucar, K. Synchrotron-Radiation-Based Determination of Xe *L*-Subshell Coster−Kronig Yields: A Reexamination via High-Resolution X-ray Spectroscopy. *Phys. Rev. A* **2010**, *81*, 012501.
(13) Wöhrle, D.; Pomogailo, A. D. *Metal Complexes and Metals in Macromolecules: Synthesis, Structure, and Properties*; Wiley-VCH: Weinheim, Germany, 2003.
(14) Winter, B.; Aziz, E. F.; Hergenhahn, U.; Faubel, M.; Hertel, I. V. Hydrogen Bonds in Liquid Water Studied by Photoelectron Spectroscopy. *J. Chem. Phys.* **2007**, *126*, 124504.
(15) Aziz, E. F. The Solvation of Ions and Molecules Probed via Soft X-ray Spectroscopies. *J. Electron. Spectrosc. Relat. Phenom.* **2010**, *177*, 168−180.
(16) Aziz, E. F.; Freiwald, M.; Eisebitt, S.; Eberhardt, W. Steric Hindrance of Ion−Ion Interaction in Electrolytes. *Phys. Rev. B* **2006**, *73*, 075120.
(17) Bergmann, N.; Bonhommeau, S.; Lange, K. M.; Greil, S. M.; Eisebitt, S.; de Groot, F.; Chergui, M.; Aziz, E. F. On the Enzymatic Activity of Catalase: An Iron L-Edge X-ray Absorption Study of the Active Centre. *Phys. Chem. Chem. Phys.* **2010**, *12*, 4827−4832.
(18) Aziz, E. F.; Ottosson, N.; Bonhommeau, S.; Bergmann, N.; Eberhardt, W.; Chergui, M. Probing the Electronic Structure of the Hemoglobin Active Center in Physiological Solutions. *Phys. Rev. Lett.* **2009**, *102*, 068103.
(19) Aziz, E. F.; Rittmann-Frank, M. H.; Lange, K. M.; Bonhommeau, S.; Chergui, M. Charge Transfer to Solvent Identified Using Dark Channel Fluorescence-Yield L-Edge Spectroscopy. *Nat. Chem.* **2010**, *2*, 853−857.
(20) Seidel, R.; Ghadimi, S.; Lange, K. M.; Bonhommeau, S.; Soldatov, M. A.; Golnak, R.; Kothe, A.; Könnecke, R.; Soldatov, A.; Thürmer, S.; Winter, B.; Aziz, E. F. Origin of Dark-Channel X-ray Fluorescence from Transition-Metal Ions in Water. *J. Am. Chem. Soc.* **2012**, *134*, 1600−1605.
(21) Panzer, D.; Beck, C.; Hahn, M.; Maul, J.; Schonhense, G.; Decker, H.; Aziz, E. F. Water Influences on the Copper Active Site in Hemocyanin. *J. Phys. Chem. Lett.* **2010**, *1*, 1642−1647.
(22) Thompson, A. C.; Attwood, D. T.; Gullikson, E. M.; Howells, M. R.; Kortright, J. B.; Liu, Y.; Robinson, A. L.; Underwood, J. H.; Kim, K.-J.; Kirz, J.; Lindau, I.; Williams, G. P.; Pianetta, P.; Winick, H.; Scofield, J. H. *X-ray Data Booklet*, 3rd ed.; Lawrence Berkeley National Laboratory, University of California: Berkely, CA, 2009.
(23) Jaklevic, J.; Kirby, J. A.; Klein, M. P.; Robertson, A. S.; Brown, G. S.; Eisenberger, P. Fluorescence Detection of EXAFS - Sensitivity Enhancement for Dilute Species and Thin-Films. *Solid State Commun.* **1977**, *23*, 679−682.
(24) Degroot, F. M. F.; Arrio, M. A.; Sainctavit, P.; Cartier, C.; Chen, C. T. Fluorescence Yield Detection - Why It Does Not Measure the X-ray-Absorption Cross-Section. *Solid State Commun.* **1994**, *92*, 991−995.
(25) Troger, L.; Arvanitis, D.; Baberschke, K.; Michaelis, H.; Grimm, U.; Zschech, E. Full Correction of the Self-Absorption in Soft-Fluorescence Extended X-ray-Absorption Fine-Structure. *Phys. Rev. B* **1992**, *46*, 3283−3289.
(26) Achkar, A. J.; Regier, T. Z.; Wadati, H.; Kim, Y. J.; Zhang, H.; Hawthorn, D. G. Bulk Sensitive X-ray Absorption Spectroscopy Free of Self-Absorption Effects. *Phys. Rev. B* **2011**, *83*, 081106.
(27) Crasemann, B. *Atomic Inner-Shell Physics*; Plenum Press: New York, 1985.
(28) Sarma, D. D.; Sr, B.; Cimino, R.; Carbone, C.; Sen, P.; Roy, A.; Chainani, A.; Gudat, W. Importance of Dynamical Effects in Determining the Auger Spectral Shape: $L_{23}-M_{45}M_{45}$ Spectra of Fe, Co, and Cu. *Phys. Rev. B* **1993**, *48*, 6822−6831.

(29) Zaanen, J.; Sawatzky, G. A. Strong Interference between Decay Channels and Valence-Electron Rearrangements in Core-Hole Spectroscopy. *Phys. Rev. B* **1986**, *33*, 8074−8083.
(30) Lange, K. M.; Konnecke, R.; Ghadimi, S.; Golnak, R.; Soldatov, M. A.; Hodeck, K. F.; Soldatov, A.; Aziz, E. F. High Resolution X-ray Emission Spectroscopy of Water and Aqueous Ions Using the Microjet Technique. *Chem. Phys.* **2010**, *377*, 1−5.
(31) Lange, K. M.; Konnecke, R.; Soldatov, M.; Golnak, R.; Rubensson, J. E.; Soldatov, A.; Aziz, E. F. On the Origin of the Hydrogen-Bond-Network Nature of Water: X-ray Absorption and Emission Spectra of Water−Acetonitrile Mixtures. *Angew. Chem., Int. Ed.* **2011**, *50*, 10621−10625.
(32) Duda, L. C.; Nordgren, J.; Drager, G.; Bocharov, S.; Kirchner, T. Polarized Resonant Inelastic X-ray Scattering from Single-Crystal Transition Metal Oxides. *J. Electron. Spectrosc. Relat. Phenom.* **2000**, *110* (1−3), 275−285.